General Concept of the EMG Controlled Bionic Hand

Adam Pieprzycki*, Daniel Król

University of Applied Sciences in Tarnow, Department of Computer Sciences, Mickiewicza 8, 33-100 Tarnow, Poland

Article history:
Received 7 January 2020
Received in revised form
12 May 2020
Accepted 12 May 2020
Available online 9 June 2020

Abstract
The article presents a general concept of a bionic hand control system using multichannel EMG signal, being under development at present. The method of acquisition and processing of multi-channel EMG signal and feature extraction for machine learning were described. Moreover, the design of the control system implementation in the real-time embedded system was discussed.

Keywords: EMG, neural-networks, machine-learning, Fourier Transform, Hilbert-Huang Transform, Hodgkin-Huxley model

Introduction

Electromyographic (EMG) signals are electro-physiological signals originating in muscles. They appear in response to muscle stimulation by electric potential coming from the nervous system [1]. Responsible for the stimulus are motor neurons α located on *the anterior grey column (anterior cornu)*. The integration of the nerve centres results in action potentials, which are transduced to the muscles via peripheral nerves. This nerves end in synapses connecting them to the muscle cells, thus creating neuromuscular junctions. When action potential acts upon these axon terminals, they release a neurotransmitter acetylcholine () and the synaptic transmission begins. Next, the acetylcholine binds to the nicotinic receptors on the postsynaptic membrane, leading to a depolarization of the muscle cell. The increase in voltage inside the cell (disturbance of the resting potential) leads to the temporary change of the potential difference on both sides of the muscular membrane. Then, sodium channels open, and when the intracellular potential reaches approx. +20 mV (fig. 1), the transport of sodium ions into the cell stops and potassium ions are moved outside the cell. The process spreads from the neuromuscular junction to the neighbouring areas. The entire mechanism is called a Na^+/K^+-ATPase, Na^+/K^+ pump or sodium–potassium pump.

Taking the contraction of a muscle into consideration, it is worth noting that after the end plate potential and the action potential have been generated, the potential inside the muscles spreads towards the cells alongside T-tubules. Additionally, Ca^{2+} is released from the vesicles of the sarcoplasmic reticulum and its diffusion to the thick and thin filaments takes place. Ca^{2+} binds to the Troponin C and the places where actin binds myosin are exposed. Subsequently, the transverse connections between actin and myosin are created and the thin filaments slide on the thick ones causing the shortening of the fibre. During the relaxation, the Ca^{2+} ions are pumped back to the sarcoplasmic reticulum, and then they unbind from the Troponin and the interaction between actin and myosin stops [2].

Table 1. Estimated concentration of ions in the intracellular and extracellular fluid inside the muscle fibres of mammals [mmol/l] [1, 2]

Ions	Intracellular fluid (cytosol)	Extracellular fluid
K^+	140–150	4–5
Na^+	10–14	140–150
Cl^-	4–6	100–125
HCO_3^-	8–10	27–28
Mg^{2+}	10–30	1–1,5
PO_4^{3-}	60	2
Ca^{2+}	10^{-4}	2,5

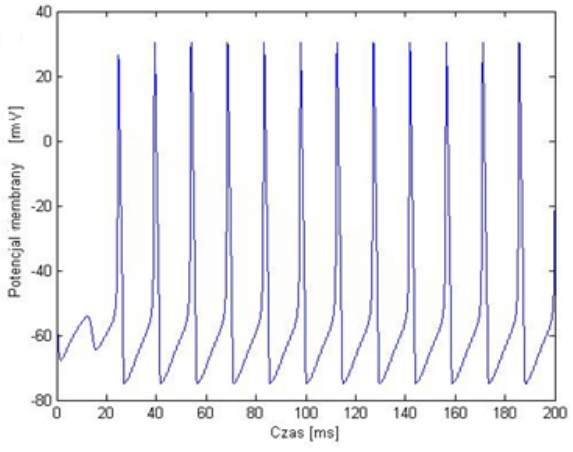

Figure 1. Representative changes of the membrane potential [3] according to the Hodgkin-Huxley model

*Corresponding author: a_pieprzycki@pwsztar.edu.pl

The electromyographic signal caused by the movement of ions can be registered on the skin as a result of temporal and spatial addition of action potentials of all active action units inside the area where the potentials can be registered by the electrodes [1]. EMG signals may also be registered with the help of the needle electrodes inserted into the muscle, but because it is a rather invasive method, the sEMG (*surface electromyography*) has been chosen for the initial stage of the research. This method has a lot of limitations because only the bioelectrical activity of the muscles located near the surface of the skin can be measured [4].

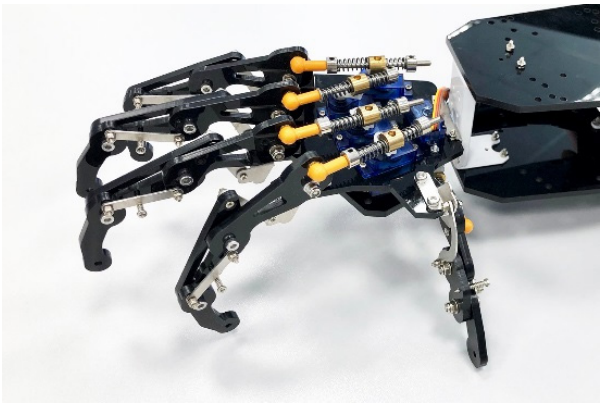

Figure 2. Bionic hand [5]

Because a bionic hand that has been used is a relatively simple (although the plan is to increase its functionality to the standard offered by the medical solutions of SaeboGlove/Flex class or similar [6]) DFRobotBionic Robot Hand [5] (fig. 2), the sEMG sensors, placed on the skin in accordance with the SENIAM [7] (*The European Recommendations for Surface Electromyography*) guidelines, have been used.

Aquisition of the sEMG signals

Among the nineteen muscles of the forearm, ten of them are responsible for flexing and extending the metacarpophalangeal and the interphalangeal joints of the fingers II-V and the thumb. Such selection of functions of the muscle stems from the design of the simple bionic hand that has been used (fig. 2). EMG signals have been obtained with the use of eight electrodes tasked with registering sEMG signals coming from:

1. The palmaris longus muscle
2. The flexor digitorum superficialis
3. The extensor digitorum
4. The extensor digiti minimi
5. The extensor indicis
6. The extensor pollicis brevis
7. The extensor pollicis longus

Placement of the electrodes

The eight electrodes measuring the signals on the surface of the skin have been placed in the middle of the forearm, as shown in figure 3. The placement of the electrodes has been carefully chosen—they have been placed above a chosen muscle, which may influence the precision of both the processing of EMG signals and machine learning algorithms of recognizing hand gestures [8].

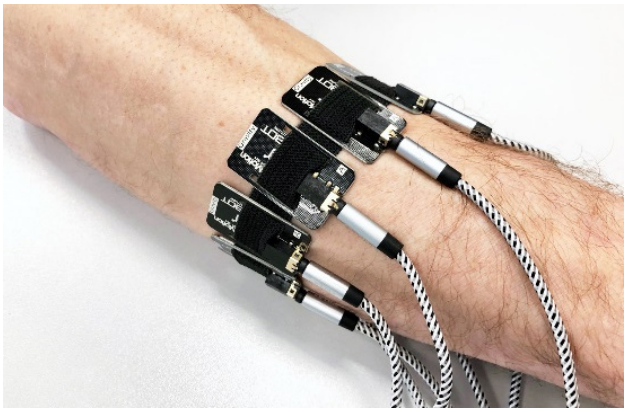

Figure 3. Placement of eight sEMG sensors around the forearm

Gestures

Because of the bionic hand available, 22 gestures based on bending and straightening of the fingers have been considered, including:

– Bending five fingers individually from the rest position (including open hand (fig. 4) and clenched fist (fig. 5), paper (as in the hand game – thumb inside)

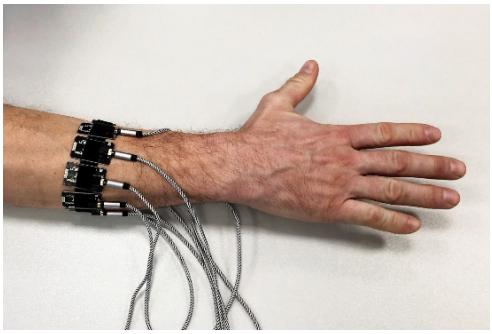

Figure 4. An open hand gesture

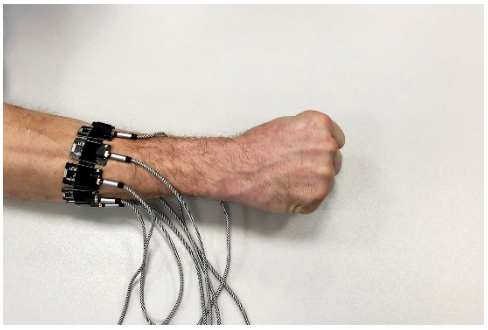

Figure 5. A closed hand gesture

– straightening the fingers from a closed hand position – individual fingers
– an OK gesture – the so-called violin (Figure 6)

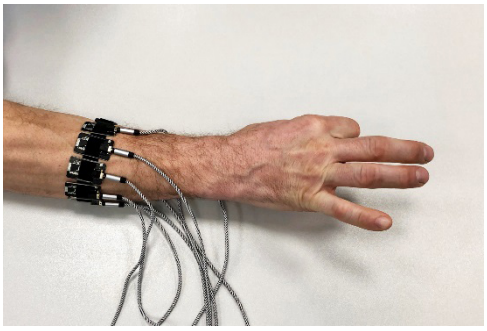

Figure 6. An OK gesture (pliers)

– a grab gesture using mittens – the so called lizard
– a pencil-holding gesture
– a call me gesture
– a V gesture – the co called scissors
– a horns gesture – 2 types
– a hand-counting gesture, including shooting and pointing gesture (Figure 7)

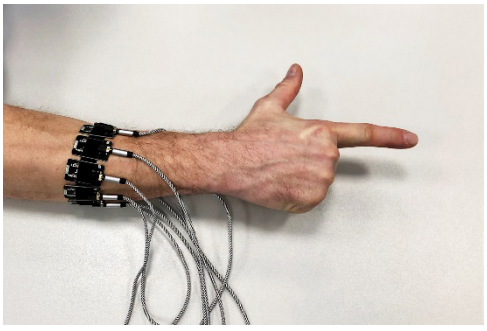

Figure 7. A hand-counting, pointing gesture.
a mug-holding gesture (Figure 8)

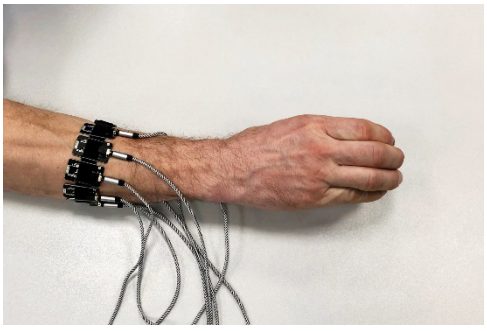

Figure 8. A mug-holding gesture

Tools and Methods

An evaluation board LPCXpresso with an LPC1347 [9] microcontroller was used in the acquisition of electromyographic signals in the initial phase of the research. The system is equipped with, among others, a 32-bit ARM Cortex-M3 core (clocked at 72 MHz) and a 12-bit successive-approximation analog to digital converter (ADC) with an 8-channel multiplexer and a hardware sequencer that switches the measuring channels. With the correct oversampling of the measured signal, this solution allows interpreting obtained data, as if they were subjected to analog-to-digital processing in eight independent converters. Surface EMG sensors of the DFRobot Gravity OYMotion type are connected into specific ADC multiplexer ports. Every sensor consists of a triple measuring electrode module and a measuring amplifier module with a gain of 60 dB. The LPC1347 module has an integrated USB 2.0 interface controller. The processed data are saved on a circular buffer and then transmitted through the USB interface to the main application. It is a classical solution that allows for a constant acquisition and transmission of the signal. The aforementioned application was implemented in the C++ language with the use of a Qt framework [10] (Figure 9). The software will allow for visualizing the measured EMG signals in real time and saving them in a multi-channel WAVE format.

To extract certain qualities of the EMG signal, the Fourier and Hilbert-Huang transforms (HHT) were utilized, using the Matlab environment. With the use of the same computing environment, that is Machine Learning Toolbox, there are plans of implementing and training a convolutional neural network (CNN). 22 gestures (finger-movements) have been differentiated and identified. The next step will be a conversion of the implemented and trained neural network into a CMSIS-NN library [11] (Figure 10), which is dedicated to processors with the ARM Cortex-M core. For the purpose of controlling the bionic hand in real time with the use of the neural network [12], a build-in system based on a microcontroller with more computing power than that used for preliminary tests will be necessary to use. The real-time controlling system is planned to be implemented on a system with an ARM Cortex-M7 core (e.g. i.MX RT1050, 600 MHz). In the next stage of research, it is planned to examine the possibilities of optimizing and implementing the neural network in a smaller, and cheaper, system with an ARM Cortex-M4 (e.g. LPC54628, 220 MHz) or an ARM Cortex-M33 (e.g. LPC55s69, 2 cores 150 MHz) core.

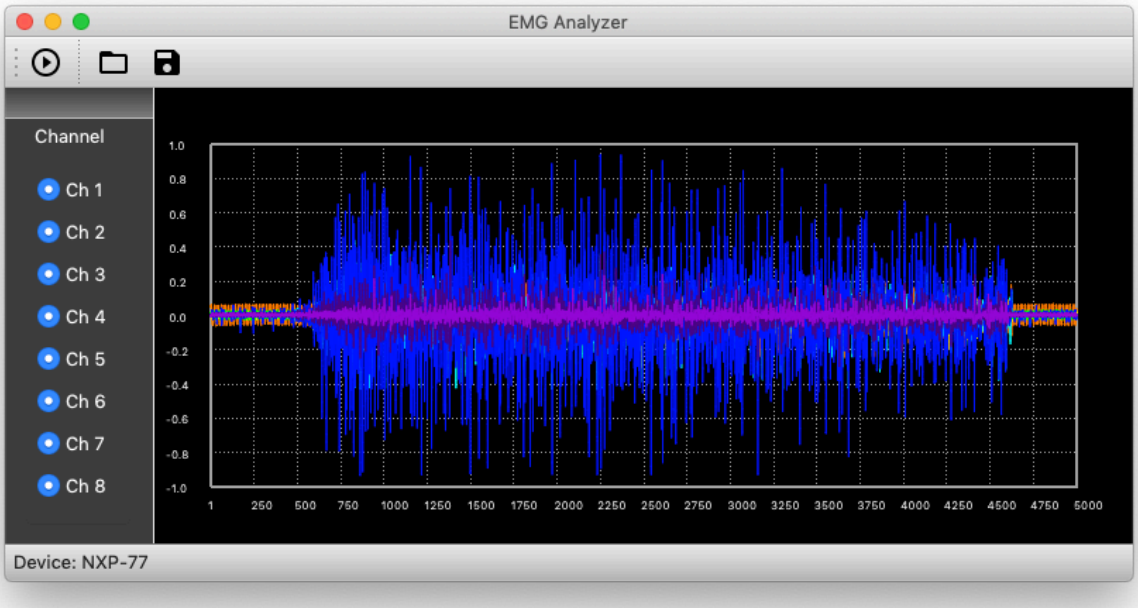

Figure 9. A window-view of the developed application during acquisition of a 8-channel EMG signal

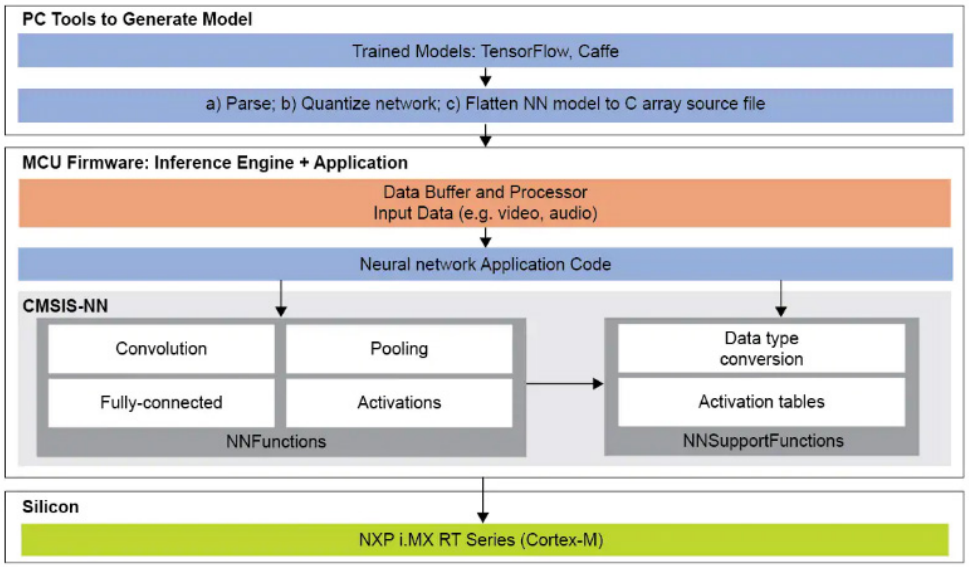

Figure 10. The conversion of a neural Network to a CMSIS-NN library [11]

Measuring problems and artifacts

Due to the type of measurements, it is crucial to maintain their reliability and repeatability. For this reason, the precise positioning of the sEMG sensors is required. Any difficulties in positioning the sensors in an anatomically correct way were minimized due to their permanent arrangement in the "ring-bracelet" configuration. It allowed placing them on the forearm in a repetitive way [8]. It is worth noting that during the sEMG measurement phase, it is possible for certain errors to occur due to the appearance of harmonic frequencies of the electrical network (50 Hz), which can be easily filtered out.

sEMG signal analysis

Table 2. The sEMG module acquisition parameters

Settings	Values
Number of sEMG channels (sensors)	8
Range of analysed frequencies	1 – 1024 Hz
Signal amplification	1000
Sampling frequency	2048 Hz
Signal acquisition time	5 s

For the analysis of non-linear and non-stationary phenomena, such as biomedical signals, in addition to well-known frequency analysis methods (e.g. Fourier transforms), time-frequency signal analysis methods should also be utilized [13]. Due to the non-stationary nature of biomedical signals, we mostly use the Short-time Fourier transform (STFT), the wavelet transform, Wigner-Ville transformations, transformations belonging to the so-called Cohen class [13] or reclusive linear modeling (Kalman filters) [14]. Because in the Hilbert transform it is assumed that the signal has a form of a single but modulated sinusoidal waveform, it can also be useful for describing considered signals.

The time-frequency analysis of the Hilbert-Huang transformation method (HHT) [15] considered in this article uses an Empirical Mode Decomposition (EDM) algorithm [15], which is adaptive enough to separate the Intrinsic Mode Function (IMF) components from each other both in time and frequency. Because this transform makes it possible to determine the distribution of energy of its frequencies in the time domain, it resembles a wavelet transform.

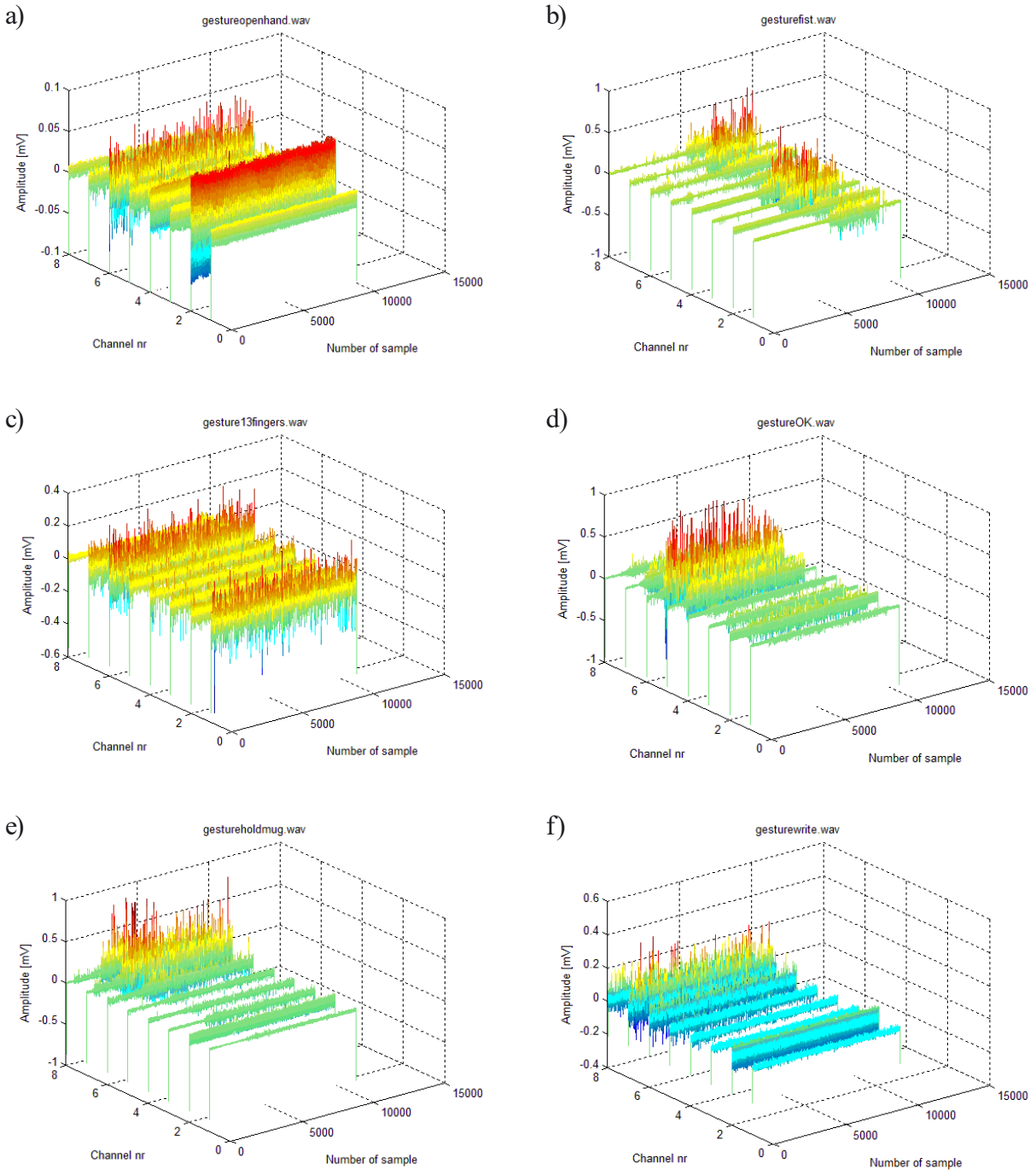

Figure 11. The amplitudes of signals of different hand gestures registered by eight sensors: a) an unclenched fist, b) a clenched fist, c) three fingers outstretched, d) an OK gesture, e) holding a mug, f) holding a pen

Figure 11 shows the amplitude values of six gestures, as registered by eight sEMG sensors.

Each of the signals received by any of the channels $x(t)$ is decomposed accordingly to the algorithm introduced by Huang and realised as:

$$x(t) = \sum_{i=1}^{K} h_i(t) + r_K(t),$$

where: $h_i(t)$ – a function, which might bea component of IMF, $r_K(t)$– residual signal.

The process of finding an IMF component is approached as follows: the signal of the local mean average (the mean average of the upper and lower envelopes of the signal) is subtracted k-times, until an IMF function is found, validated by two criteria [14]:

1. the number of extrema and the number of times the signal crosses zero must be equal or the difference between them cannot be greater than 1
2. the mean values of the envelope interpolating the local

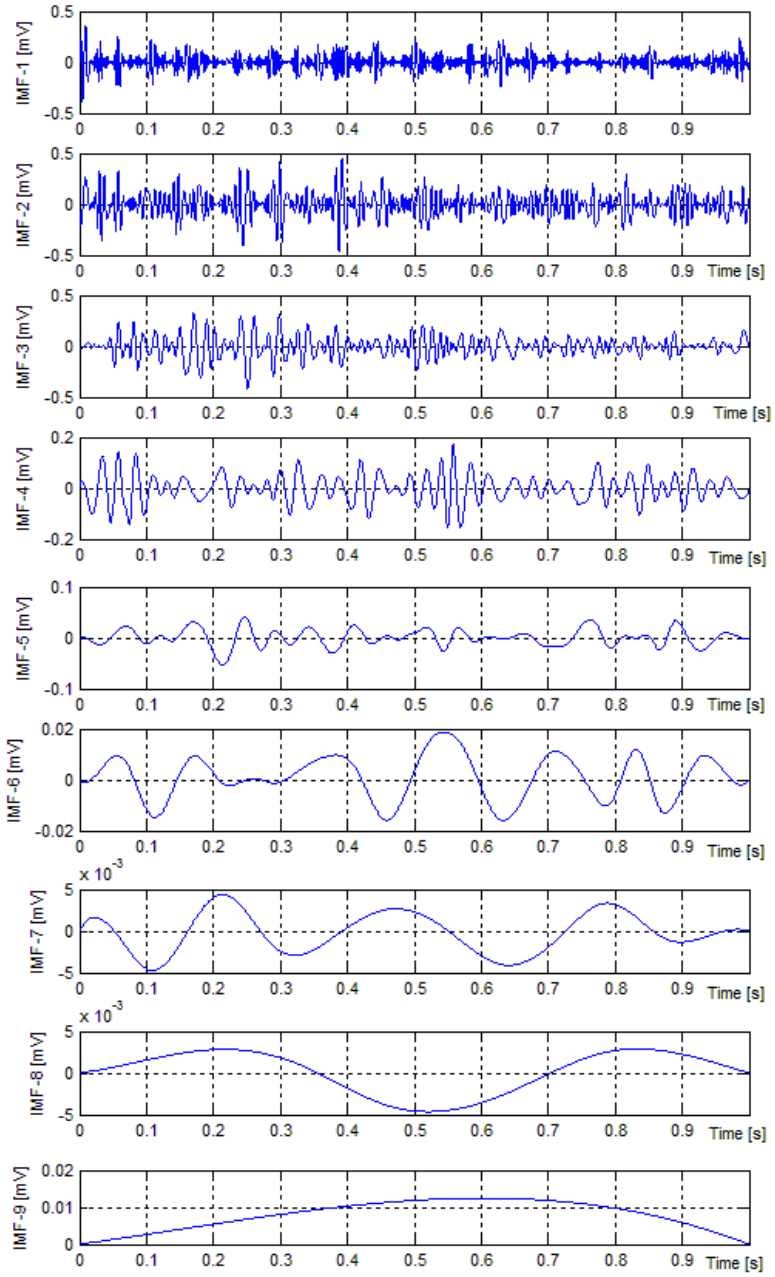

Figure 12. Decomposed IMF components for the channel no. 7

maxima and the envelope interpolating the local minima amount to 0.

The HHT algorithm is an extension of the EMD algorithm by the inclusion of the Hilbert transform. It is a transformation of time, realised as [16] [17]:

$$\hat{h}(t) = \pi^{-1} \int_{-\infty}^{+\infty} \frac{h(\tau)}{t-\tau} d\tau$$

The transform allows for stating the instantaneous values of amplitudes as well as the frequencies of the decomposed components of a signal. The use of such analysis will make isolating and pinpointing the dominating frequency in a signal possible.

The 12th figure shows an example of an EMD decomposition for the hand gesture of holding a mug (fig. 11e) taken from one of the channels (sensors) no. 7, including all the decomposed components of an IMF signal. From a five-second-long sample, data amounting for a second of making the proper gesture was extracted.

Out of the resulting IMF functions, the use of one of them [18] and four of them [19] will help with further analysis of the signal features.

Analysing the IMF components (fig. 14) leads to an observation that the first four functions have the greatest amplitude and carry the biggest amount of the signal energy.

In the analysis of the parameters of the signal, the object of the study will be the feature extraction out of four IMF in time, and it will be realised as a RMS (*Root Mean Square*) of the values of the samples [19]:

$$RMS = \sqrt{\frac{1}{N}\sum_{n=1}^{N} x_n^2}$$

The autoregressive model AR (of the 4th order) will be used as well. It incorporates the linear combination of the last four samples of each IMF component, along with the noise, in which the value of a sample can be realised as:

$$x_n = -\sum_{i=1}^{p} a_i \cdot x_{n-1} + w_n,$$

where: x_n – IMF signal samples, a_i – AR coefficients, which need to be calculated, p – the AR model order, w_n – a white noise sample, with mean average 0 and a variance σ_x^2.

In the instance of using eight channels with four IMF functions and five employed features each, each gesture has 160 features [19].

The use of feature extraction of the signal of each IMF components including the following is to be discussed [18]:

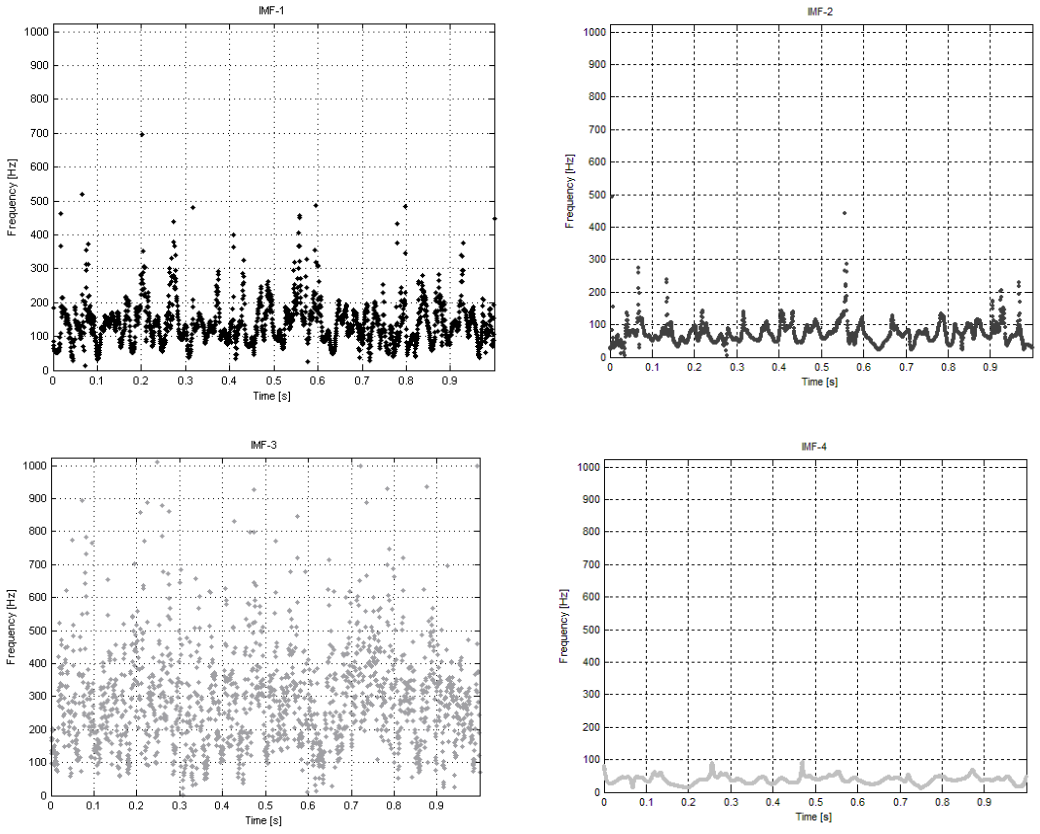

Figure 13. The time-frequency analysis of the first four IMF components

– the mean value
– standard deviation
– energy
– entropy
– the maximal value
– the minimal value
– scatter (the dispersion between the minimal and maximal values).

The described research included an additional preliminary study of the data from the whole measuring range (5sec) of the channels no. 1 and no. 7 (fig. 11e).

By analysing the amplitudes of the figures depicted on the charts (fig. 14 and fig. 15) of the first four IMF components, it can be observed that both the exact moment of the beginning of making a gesture (circa 1,3 sec after the start) and the participation level of each muscle measured by the electrodes no. 1 (fig. 14) and no. 7 (fig. 15) varied greatly.

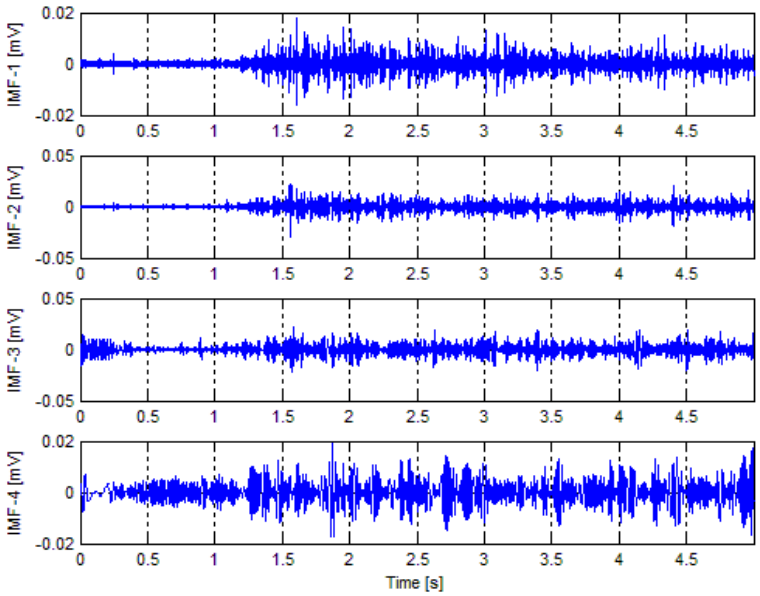

Figure 14. Four IMF components of the channel no. 1

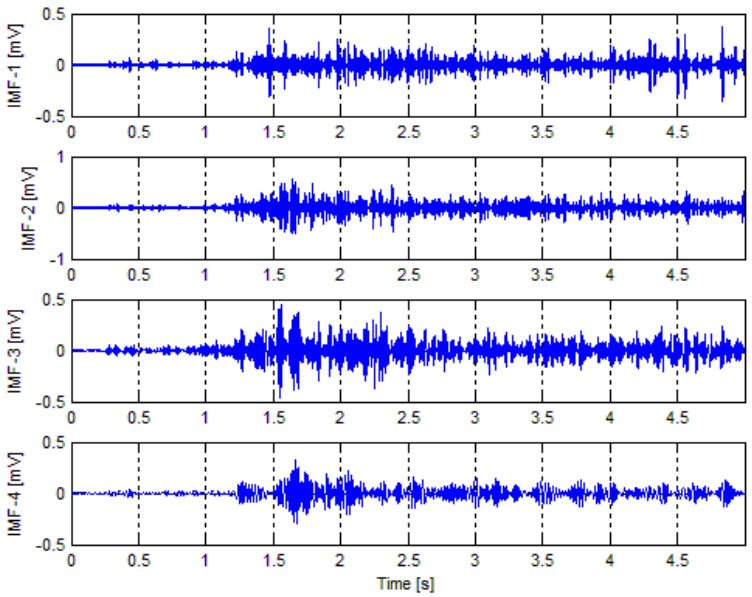

Figure 15. Four IMF components of the channel no. 7

Conclusions

The article describes the general idea behind the system of real-time control of the bionic hand. The preliminary results of the original research confirmed that there is a possibility of separating various gestures on the basis of multi-channel acquisition of the EMG signal. Moreover, the article presents a methodology of extraction of features from the 8-channel EMG signal to be used in neural network learning. The collection of samples of signals related to different gestures from several dozen people has been planned. After ,convolutional neural network has been implemented, trained and tested in the Matlab environment, it will ultimately be converted to CMSIS-NN library dedicated to the processors with the ARM Cortex-M core. In the last stage of the project, the system measuring the EMG signals on the forearm will be used to control the bionic hand.

Author Contributions

Conceptualization, Pieprzycki A. and Król D.; methodology, Pieprzycki A.; software, Król D.; validation, Pieprzycki A. and Król D.; formal analysis, Pieprzycki A.; investigation, Pieprzycki A. and Król D.; resources, Pieprzycki A.; data curation, Król D.; writing – original draft preparation, Pieprzycki A. and Król D.; writing – review and editing, Pieprzycki A. and Król D.; visualization, Pieprzycki A. and Król D.; supervision, Pieprzycki A.; project administration, Pieprzycki A.; funding acquisition, Pieprzycki A.

References

1. Błaszczyk JW. Biomechanika kliniczna. Warszawa: PZWL; 2014.
2. Murray RK, Granner DK, Rodwell VW. Biochemia Harpera. Warszawa: PZWL; 2008.
3. Chandra R. hhrun - Hodgkin Huxley model simulation for user defined input current. MATLAB Central File Exchange, [Online]. Available: https://www.mathworks.com/matlabcentral/fileexchange/46740-hhrun-hodgkin-huxley-model-simulation-for-user-defined-input-current. (accessed 10.12.2019).
4. Wołczowski A, Błędowski M, Witkowski J. System do rejestracji sygnałów EMG i MMG dla sterowania bioprotezą dłoni. Prace Naukowe Politechniki Warszawskiej. Elektronika. 2016;195(1);167-178.
5. DFRobot Bionic Robot Hand, DFRobot, [Online]. Available: https://www.dfrobot.com/product-1623.html. (accessed 2019.12.11).
6. Saebo, [Online]. Available: https://www.saebo.com/shop/saeboglove/. (accessed 2019.12.11).
7. Recommendations for sensor locations on individual muscles, SENIAM, [Online]. Available: www.seniam.org/sensor_location.htm. (accessed 07.06.2020).
8. Yoo HJ., Park H, Lee B. Myoelectric Signal Classification of Targeted Muscles Using Dictionary Learning. Sensors. 2019;19(2370):1-19. doi: https://doi.org/10.3390/s19102370
9. NXP Semiconductors, [Online]. Available: https://www.nxp.com/design/microcontrollers-developer-resources/lpc-microcontroller-utilities/lpcxpresso-board-for-lpc1347:OM13045. (accessed 07.06.2020).
10. QT Company. Qt Framework - One framework to rule all! [Online]. Available: https://www.qt.io/product/framework. (accessed 07.06.2020).
11. eIQ™ for Arm® CMSIS-NN, [Online]. Available: https://www.nxp.com/design/software/development-software/eiq-ml-development-environment/eiq-for-arm-cmsis-nn:eIQArmCMSISNN. (accessed 07.06.2020).
12. Geron A. Uczenie maszynowe z użyciem Scikit-Learn i Tensorflow. Gliwice: Helion; 2018.
13. Zieliński TP. Cyfrowe przetwarzanie sygnałów. Warszawa: WKŁ; 2007.
14. Gawędzki W, Socha M, Sławik P. Dekompozycja sygnałów EEG w dziedzinie czasu przy zastosowaniu transformacji Hilberta-Huanga HHT. Przegląd Elektrotechniczny. 2015;91(5):33-36.
15. Huang NE, Shen Z, Long SR, Wu MJ, Shih HH, Zheng Q, Yen NC, Tung CC, Liu HH. The Empirical mode decomposition and the Hilbert Spectrum for nonlinear and non-stationary time series analysis. Royal Society of London Proceedings Series A. 1998; 454(1971):903-998. doi: https://doi.org/10.1098/rspa.1998.0193.
16. Feldman M. Hilbert Transform Application in Mechanical Vibration. Wiley; 2011.
17. Huang NE, Shen SSP. Hilbert-Huang Transform and Its Applications. Singgapore: World Scientific; 2005.
18. Kukker A, Sharma R, Malik H. Forearm movements classification of EMG signals using Hilbert Huang transform and artificial neural networks. Materiały konferencyjne 2016 IEEE 7th Power India International Conference (PIICON); 2016 Nov 25-27; Bikaner, India: IEEE; 2016. doi: https://doi.org/10.1109/POWERI.2016.8077417.
19. Ruiz-Olaya AF, López-Delis A. Surface EMG Signal Analysis Based on the Empirical Mode Decomposition for Human-Robot Interaction. Materiały konferencyjne Symposium of Signals, Images and Artificial Vision - 2013: STSIVA - 2013; 2013 Sep 11-13; Bogota, Colombia; 2013. doi: 10.1109/STSIVA.2013.6644943.
20. Tan A. Hilbert-Huang Transform. MATLAB Central File Exchange, [Online]. Available: https://www.mathworks.com/matlabcentral/fileexchange/19681-hilbert-huang-transform. (accessed: 31.12.2019).